Spectroscopic Studies of RV Tau and Related Objects

A Synopsis of the Thesis to be Submitted to the Mangalore University
for the Award of the Degree of Doctor of Philosophy in Physics

Submitted by

S. Sumangala Rao

Under the Supervision of
Prof. Sunetra Giridhar

Indian Institute of Astrophysics
Bangalore - 560034, INDIA

April 2012

Contents :

a) Introduction ——— Pages 2 to 4

b) Stellar evolution for a $1M_{\odot}$ star —— Pages 4 to 7

c) Scientific goals —- Pages 7 to 8

d) Selection of the sample, Observations and Data Reduction — Pages 8 to 12

e) Measurement of equivalent widths and definition of abundance — Pages 12 to 13

f) Atmospheric Models, codes and atomic data used — Pages 13 to 15

g) Results —- Pages 15 to 22

h) Summary of the work done — Pages 22 to 23

i) References and List of Publications—- Pages 23 to 25

INTRODUCTION

Considerable theoretical and observational interest has in recent years been focused on asymptotic giant branch (AGB) stars but much remains mysterious about them. The AGB phase is enjoyed by low and intermediate mass stars (approximate mass range 0.8 to $8M_{\odot}$). It is in this phase that a star experiences extensive internal nucleosynthesis whose fruits are dredged to the stellar surface (see Herwig 2005). Furthermore, mass-loss ensures that the products of nucleosynthesis are dispersed into the circumstellar and subsequently the interstellar environment. Thus, AGB stars are likely major contributors of Li, C, N, F and *s*-process elements among others to Galactic chemical evolution (Romano et al. 2010).

Observational validation of theoretical investigations of how AGB stars achieve internal nucleosynthesis, dredge-up and mass-loss are generally hampered by the fact that the more evolved and more interesting of these stars have low temperature atmospheres and therefore spectra replete with dense and complex molecular lines. Although these spectra have been analysed by a few stellar spectroscopists, the abundance studies are generally limited to very few elements and isotopic ratios.

The AGB phase of stellar evolution concludes with a rapid phase of evolution to the tip of the white dwarf cooling track. This post-AGB (PAGB) phase takes a star in a few thousand years or so from a cool AGB star to a very hot central star of a planetary nebula and onto a white dwarf cooling track. Along this track, the star's spectrum is amenable to straightforward abundance analysis and thus offers apparently a way to infer the abundance changes brought by the PAGB star's AGB progenitor. This inference is, of course, dependent on the assumption that the composition of an AGB star is exactly preserved by the PAGB star. Observations of certain PAGB stars show that this is a false assumption. For example, several PAGB stars show abundance anomalies correlated with the condensation temperature (T_C)[1] for dust grains to condense out of gas of normal composition (see Van Winckel 2003 for a review) – a process we refer to as 'dust-gas winnowing'. Other PAGB candidate stars show abundance anomalies correlated with the ionization potential of the neutral atoms (Rao and Reddy 2005) – a process we refer to as 'the FIP effect'.

RV Tauri stars are pulsating variables located in the instability strip along with the Cepheids but at relatively lower luminosities. The location of RV Tauri vari-

[1] **The condensation temperature T_C is the temperature at which half of a particular element in a gaseous environment condenses into dust grains. Condensable elements refer to the refractories like Ti, Ca, Sc and the s-process elements which readily condense into dust grains because of their high T_C.**

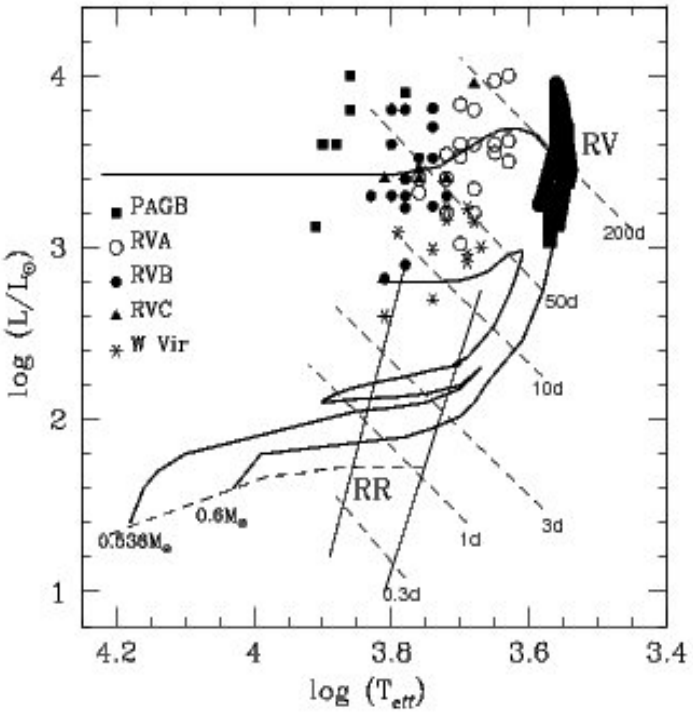

Figure 1: H-R diagram showing the location of the population II and the classical instability strip, lines of constant period and the theoretical evolutionary tracks for a 0.536 and 0.6$M_{\odot}$ star. The location of the well studied RV Tauri stars, W Vir variables and PAGB stars have been shown. This figure is an adaptation from Gingold (1985).

ables as well as our program RV Tauri stars have been plotted in Figure 1. Their characteristic light curve shows alternating deep and shallow minima with a formal period (time elapsed between two consecutive deep minima) of 30-150d. Figure 2 shows a typical light curve of a RV Tauri star: AC Her.

Because of intersection of evolutionary tracks with Pop II instability strip, post-AGB stars also contain variable stars such as RV Tauri's, W Virginis variables and some SRD's. Photometrically there are two types of RV Tauri stars (Kukarkin, Parenago and Kholopov 1958): RVa stars show a quasi- constant brightness at maximum light whereas RVb stars exhibit a longer term variation in brightness with a period of about 600-1500 days. This variation is often ascribed to an orbital variation with the star's light modulated by dust in the dusty circumstellar envelope (Pollard et al. 1996). Preston et al.(1963) classified RV Tauri variables spectroscopically into RVA, RVB and RVC. RVA which have spectral type G-K and near light minimum show TiO bands of abnormal strength, RVB are weak-

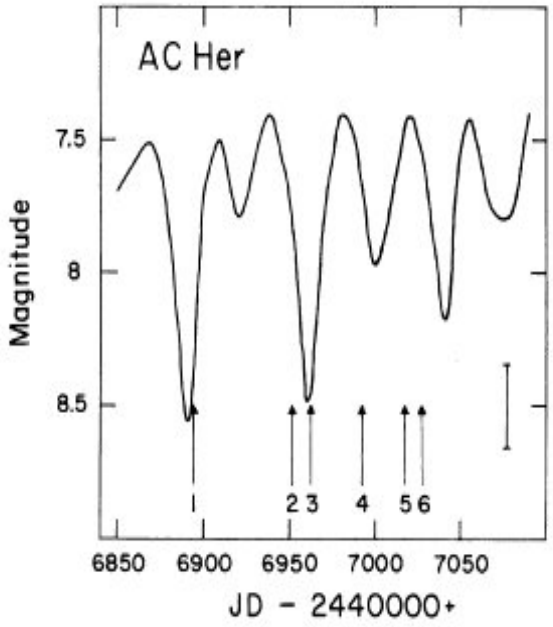

Figure 2: Typical light curve of a RV Tauri star (AC Her) taken from Nook et al. (1990).

lined objects of spectral type F and exhibit strong CN and CH bands at light minimum, RVC are metal-poor objects and the CN and CH bands are weaker or absent at all phases.

With the detection of RV Tauri stars in the LMC by Alcock et al. (1998), their location on the high luminosity end of the population II instability strip was confirmed. With the known distance modulus of the LMC, an absolute magnitude of -4.5 was estimated for RV Tauri variables with fundamental periods (time elapsed between a deep and a shallow minima) of about 50 days using the calibrated P-L-C (Period-Luminosity-Colour) relation. The detection of IR fluxes (Jura 1986) and the determination of high luminosities (Alcock et al. 1998) supports the idea that these stars are in the PAGB phase evolving towards the blue in the H-R diagram.

Stellar evolution after the Main-Sequence for a 1 $M_\odot$ star

Figure 3 shows the evolution of a $1M_\odot$ star in the H-R diagram starting from the ZAMS (Zero Age Main Sequence). Once the hydrogen is exhausted in the core the star leaves the main-sequence. The helium rich core contracts and the hydrogen fusion starts in a shell surrounding the core, simultaneously the outer layers expand and becomes convective due to an increase in the opacity. The

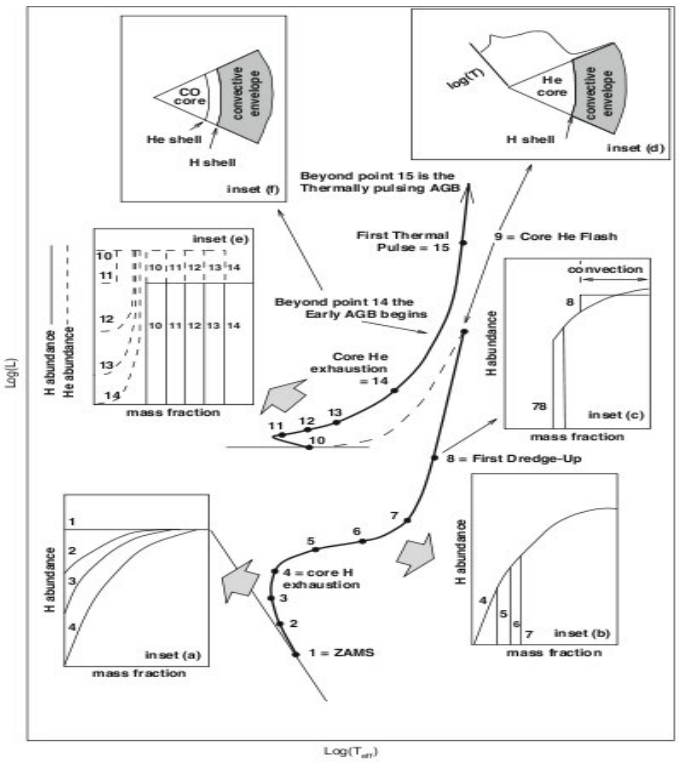

Figure 3: Evolution of a $1M_{\odot}$ in the H-R diagram starting from the ZAMS upto the thermally pulsing AGB phase (Lattanzio and Boothroyd 1997).

luminosity increases, surface temperature decreases and the star becomes a red giant for the first time.

During it's ascent on the Red Giant Branch (RGB), the convective envelope moves inward mixing the outer layers with the internal matter that has experienced partial hydrogen burning. This mixing event is called the FDU (First Dredge Up). The material processed by the CNO cycle of hydrogen fusion is carried to the star's surface. The result is increase in ^{4}He by 5%, ^{14}N by 30% and decrease in ^{12}C by 20%. During the ascent on the RGB, the He core continues to contract and becomes electron degenerate. The RGB life time terminates when the central temperature reaches 100 million degrees Kelvin which is sufficient to ignite He in the core. Now the 3-α reactions take place resulting in violent He ignition-core He flash. After the main He flash the He burning luminosity oscillates before settling to the quiescent core-He burning.

Following the core He flash the star moves to the Horizontal Branch (HB) where it burns He in a convective core and H in a shell which provides most of the luminosity. He burning in the core increases the fraction of ^{12}C and ^{16}O. But in the case of more massive stars the He core remains non-degenerate and He

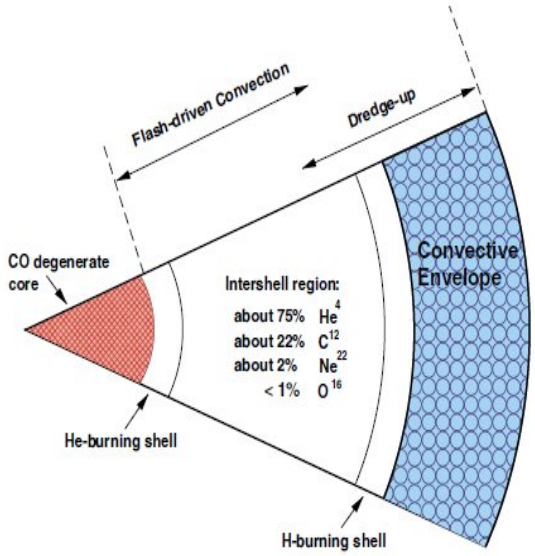

Figure 4: Structure of an AGB star (Karakas 2010).

burns quiescently without undergoing the core He shell flash. Figure shows the evolution of a $5M_{\odot}$ star. Once the He in the core gets exhausted the star ascends the giant branch for the second time – Asymptotic Giant Branch (AGB). The star now becomes an AGB star which has a degenerate CO core, He fusing shell, H fusing shell and a H-rich convective envelope. Figure 4 shows the schematic structure of an AGB star.

The AGB is divided into two regimes:

Early AGB phase (E-AGB): During this E-AGB phase which takes about 90% of the total AGB life-span, the AGB star burns He quiescently in a narrow shell surrounding the electron degenerate CO core.

Thermally Pulsing AGB phase (TP-AGB): When the helium burning is extinct, the energy production is taken over by episodes of quiescent hydrogen-shell burning also known as the interpulse phase interrupted by instabilities of the helium shell. The ashes of the hydrogen-shell increase the thickness of the hydrogen depleted region until the next thermal pulse occurs. During every thermal pulse or an instability also called the on-phase, the helium shell burns with luminosities upto $10^8 L_{\odot}$ for a few hundred years. This energy is utilised in driving a convective zone in the helium-intershell. When the helium shell finally dies down (power-down phase), the energy from the thermal pulse causes the expansion of the whole star and the hydrogen shell is pushed to cooler regions and extinguished. At this time the convective envelope moves inwards and dredges up the products of hydrogen and helium shell burning to the surface in a process called the

Third Dredge-Up (TDU) which occurs periodically after each thermal pulse. This mechanism is responsible for producing the s-process elements as well as converting the photosphere from oxygen-rich to carbon-rich depending on the mass and metallicity of the star. After TDU, the whole star contracts and the helium shell is re-ignited and the cycle re-iterates.

When the mass of the H-rich convective envelope becomes smaller than $0.05M_{\odot}$, the stellar effective temperature starts to increase and the mass loss rate decreases and the star begins its post-AGB phase. But the post-AGB life time is very short 10^3 to 10^4 yrs and only about 326 very likely and 107 possible post-AGB candidates are listed in the Toruń catalogue of Galactic post-AGB and related objects.

Post-AGB stars serve as excellent probes to study the AGB nucleosynthesis and mass-loss as they are optically brighter, have relatively stable atmospheres and being relatively warm their spectra permit comprehensive abundance analysis of a whole range of atomic species.

Scientific Goals:

Post-AGB stars represent a crucial phase in the evolution of low and intermediate mass stars ($0.8\text{-}8M_{\odot}$) where rapid change in the surface composition of the star and its circumstellar envelope takes place.

A very small fraction of the known post-AGB objects show hard core PAGB abundance pattern i.e. the C/O larger than 1 and enhancement of s-process elements. Many of them show chemical peculiarities not caused by the nucleosynthesis. From the spectroscopic studies of a number of RV Tauri and post-AGB objects it is found that many of these show abundance anomalies due to selective depletion of condensable elements. These stars show abundance anomalies correlated with their condensation temperatures and this process is known as the dust-gas winnowing. A large fraction of these stars are found to be binaries and this depletion is thought to be occurring in a dusty circumbinary disk. Some post-AGB candidates show abundance anomalies correlated with the ionisation potential of the neutral atoms. This process is known as the FIP (First Ionisation Potential) effect.

A good fraction of post-AGB stars are neither s-process enriched nor show the effects of dust-gas separation. In our spectroscopic study of RV Tauri and post-AGB candidates, we try to find the signature of various processes that may affect the stellar composition during the course of its evolution like the initial composition of the ISM, effect of FDU (First Dredge Up), effect of thermal pulses and TDU (Third Dredge Up), effects of dust-gas winnowing and FIP effect and also try to re-define the boundary conditions (temperature, metallicity, binarity) for these processes to operate.

We propose to study the unexplored (as well as the ones lacking comprehen-

sive abundance analysis) RV Tauri stars and post-AGB objects to understand the morphological and chemical changes taking place during the late stages of stellar evolution of low and intermediate mass stars.

We have tried to enlarge the RV Tau and PAGB sample and also present a critical compilation and statistics of all these objects studied till now to understand the importance of the stellar parameters and of the conditions such as binarity on PAGB evolution. We have divided our compilations into several sub-groups such as those showing s-process enrichment, dust-gas winnowing, FIP effect and those having normal compositions.

We also explore the evolutionary link between RV Tau and PAGB stars although the latter appear to be in a more advanced stage of evolution. However there is considerable ambiguity regarding the termination of the AGB phase and the onset of the RV Tau behaviour.

While conducting the literature survey of these objects we were surprised to see different families of depletion curves. Starting with the depletion curve of R Sct with an almost precipice like fall at high condensation temperatures, the length and height of low and intermediate condensation temperature plateau show considerable variations. Then there are another set of objects with depletion curve asymptoting at higher condensation temperatures at different [X/H] level whereas the depletion curves of a few objects have many persistent outliers. An attempt has been made to explain the observed depletion curves taking into consideration conditions such as the temperature and composition of the circumstellar environment as well as the efficiency of mixing between the accreted clean gas with the atmosphere/envelope of the star.

Selection of the sample

In Figure 5 we have plotted our program RV Tauri stars and also the well known RV Tau stars (with known spectroscopic classification) in IRAS two colour diagram. The IR fluxes of known RV Tau stars have been investigated by Lloyd Evans (1985) and Raveendran (1989) who found that RV Tau stars fall in a well-defined region of the IRAS [12]-[25], [25]-[60] diagram enclosed by the limits [12]-[25] 1.0− 1.5 and [25]-[26]=0.20 − 1.0. Lloyd Evans (1999) suggested that this RV Tau box provides an alternative method of searching for such stars. In fact the photometric monitoring of IRAS sources with RV Tau like IRAS colours, K and L excesses and spectral types B-M did result in finding new samples of RV Tau objects subsequently studied by Maas et al. (2002,2005). Although a good fraction of known RV Tau stars are found in this area many well known RV Tau particularly RVB stars do not conform to these limits and have redder IRAS colours. Nevertheless this box can be used for identifying RV Tau candidates among IRAS sources with no photometry.

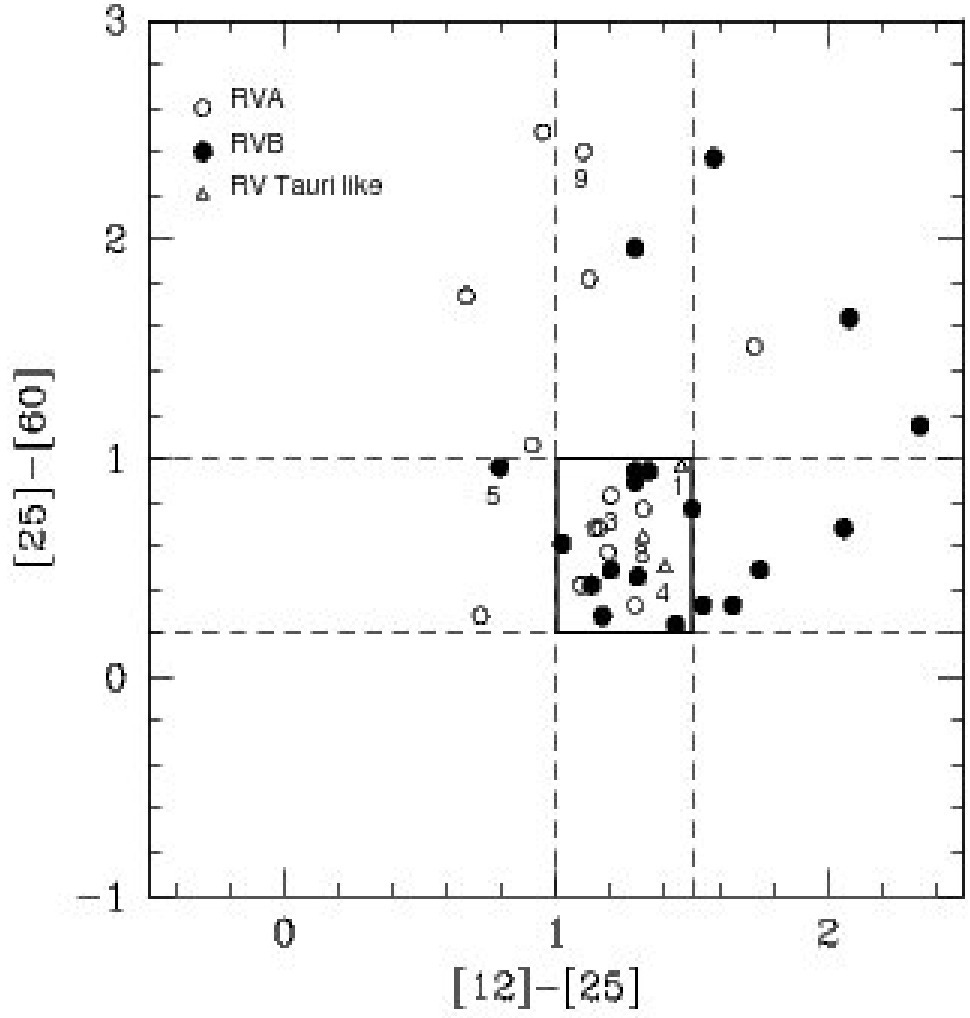

Figure 5: The IRAS colour-colour diagram showing the ”RV Tauri box”. The figure contains our program stars as well as all the well studied RV Tauri stars

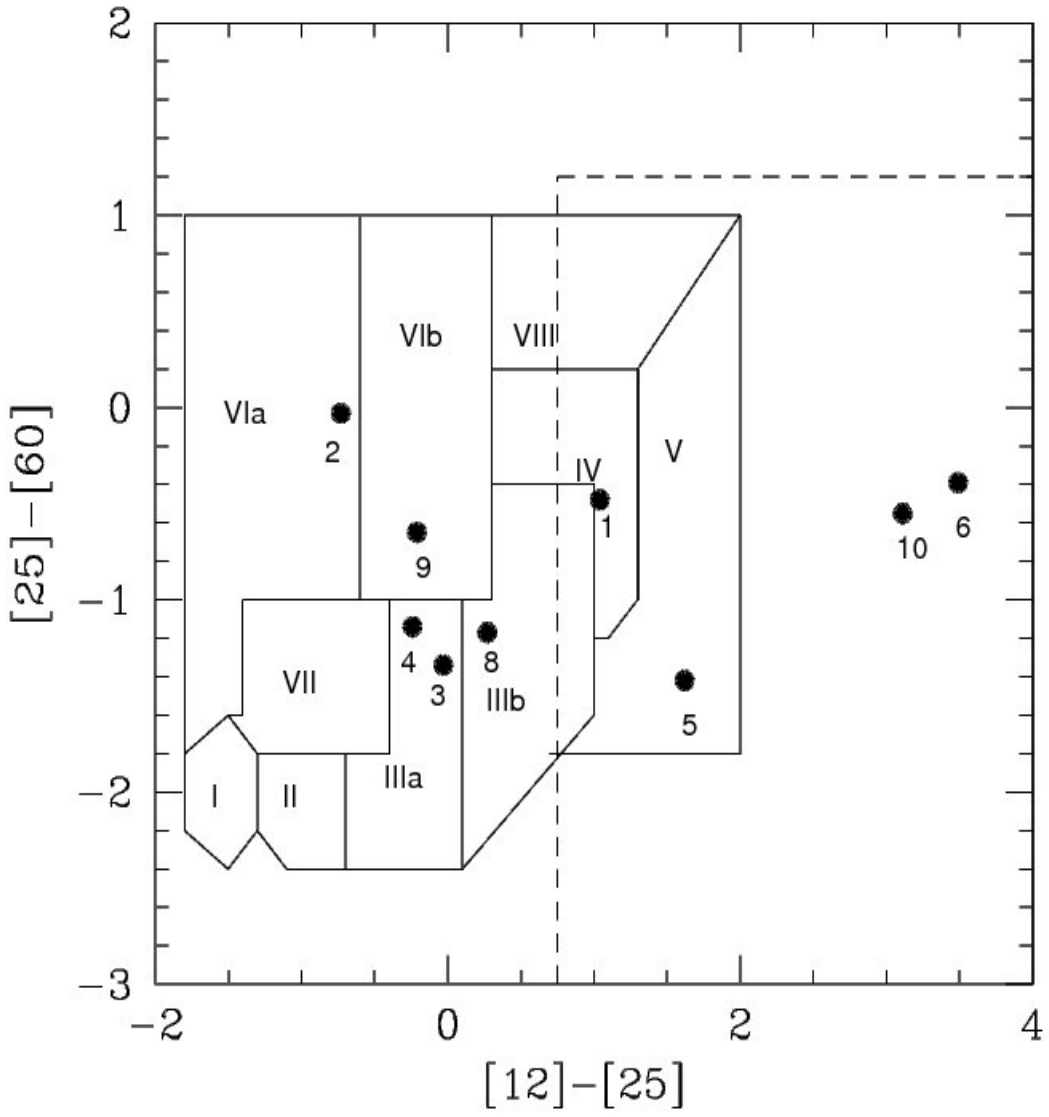

Figure 6: The location of the candidate post-AGB stars in the IRAS colour-colour diagram containing the zones and the area enclosed in the dashed line is richly populated by post-AGB's with colours like planetary nebulae.

Most of our program stars with exception of BT Lac are located in or around RV Tau box. BT Lac and a few RVA stars have IRAS colours indicating the presence of both hot and cool dust shells. The colours of RVB stars points to the existence of cooler dust shells.

The post-AGB candidates for our study were selected based on its position in the IRAS two colour diagram which has proven to be a powerful tool for identifying these stars ((van der Veen & Habing 1988; Suárez et al. 2006; Szczerba et al. 2007) as can be seen in the Figure 6.

It is known that zone 1 of IRAS two colour diagram corresponds to fluxes from stellar photospheres warmer than 2000K. The IRAS colours of Zones II-III signify the emergence and evolution of circumstellar shell (CS) produced by increasing large mass-loss at AGB. Sources at Zone IV are at the super-wind phases or slightly beyond. Zone V contains objects with only signature of cold dust shell as the mass-loss has stopped hence warm dust is not being added. The objects with detached cold CS would be seen at region VIa, while objects in zone VIb contains objects with warm as well as cold CS. The Zone VII and dashed region is dominated by PAGBs with PN like colours.

A detailed abundance analysis for 21 stars (post-AGB candidates and RV Tauri stars) have been undertaken through high resolution spectroscopy.

Observations and Data Reductions

The high resolution spectra of our program stars were obtained with the 2.34m Vainu Bappu Telescope at the Vainu Bappu Observatory (VBO) in Kavalur, India giving a resolution of 28,000 in the slitless mode (Rao et al. 2005).

The high-resolution optical spectra of fainter stars in our sample were obtained at the W.J. McDonald Observatory with the 2.7m Harlan J. Smith reflector and the Tull coudé spectrograph (Tull et al. 1995) with a resolving power of 60,000. Spectral coverage in a single exposure from this cross-dispersed echelle spectrograph is complete up to 6000Å and extensive but incomplete at longer wavelengths. A S/N ratio of 80-100 over much of the spectral range was achieved. Figure 7 shows the sample spectra of some of our program stars.

We have used the IRAF (Image Reduction and Analysis Facility) package for reducing the spectra of our program stars. IRAF is developed and distributed by the National Optical Astronomy Observatory and operates under the UNIX environment. For the wavelength calibration, emission lines are identified in the spectra of the Th-Ar source using the atlas of Th-Ar laboratory spectra. We now have the wavelength calibrated spectra of the object in the form of stellar counts versus wavelength. The stellar spectrum is then normalised to the continuum. The continuum is estimated visually, using the average of the highest points in the spectrum, from regions free of emission and absorption features.

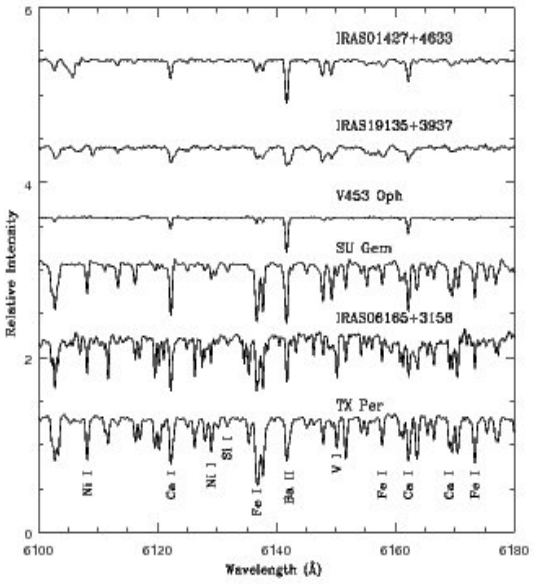

Figure 7: Sample spectra of some of our program stars presented in descending order of temperature in the 6100-6180 region

Measurement of equivalent widths

The equivalent widths of the absorption lines in the stellar spectrum of our program stars have been measured in two ways using the splot task in IRAF. One is by fitting a gaussian to the absorption line and the other by measuring the total area under the line. We have measured mostly symmetric and unblended lines in our program stars. The accuracy of the equivalent width measurements depends on the spectral type of the star, the continuum fitting and also on the spectral resolution. For the program stars of spectral type A-F the equivalent widths could be measured with accuracy of 5-8%. But for cooler stars an accuracy of 8-10% could be achieved.

Definition of Abundance and Equivalent widths

Basically abundances are usually the logarithmic number densities on a standard scale in which log ϵ(H)=12. To obtain the abundances of elements in a cosmic object the standard practice is to compare the element content in a cosmic object with the corresponding value for the Sun using the normal logarithmic abundance scale:

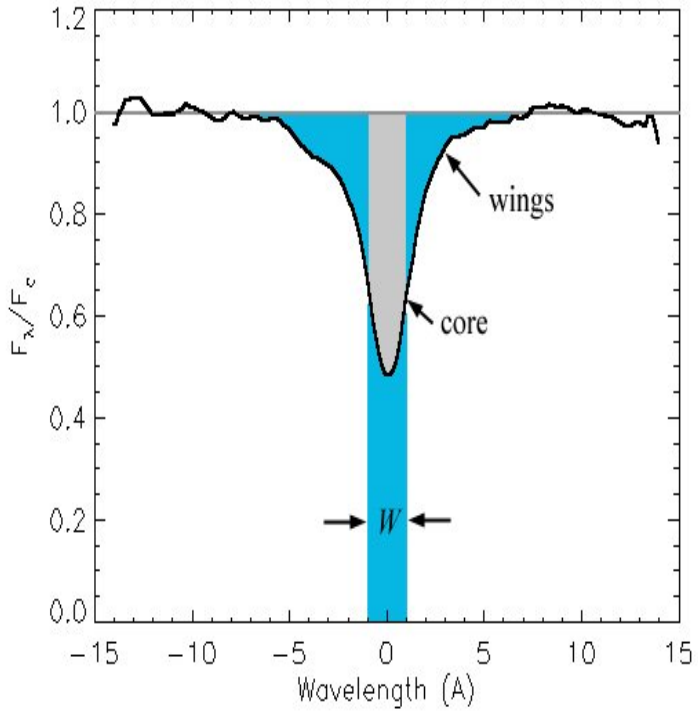

Figure 8: Equivalent Width of a spectral line

$$[X/H]=\log (N_X/N_H)_* - \log (N_X/N_H)_\odot = \log \epsilon_{X,*} - \log \epsilon_{X,\odot}.$$

To derive abundances we need to measure the line strengths for a large number of lines for the species of interest. The line strength is expressed as the equivalent width. The equivalent width is the amount of energy which is subtracted from the neighbouring continuum due to the presence of line as can be seen in Figure 8. It is measured as the area under the curve. It can be considered as a width of a black rectangle which has the same area as the stellar line.

$$W_\lambda = \int (F_C - F_\lambda)/F_C \, d\lambda = \int R_\lambda d\lambda$$

The relation between line strength and the number of absorbers and its dependence on other stellar parameters forms the basis of abundance determination methods.

Atmospheric Models and codes used for calculation of abundances

We have made use of the new grid of ATLAS09 model atmospheres avail-

able at the database of Kurucz[2]. These models are constructed based on the assumptions of LTE (Local Thermodynamic Equilibrium). The assumptions for a LTE model atmosphere are that the atmosphere is in a steady state, atmosphere is plane-parallel (the atmosphere is thin relative to the radius of the star), hydrostatic equilibrium and flux conservation.

For the abundance analysis of our program stars, we have used 2010 version of the LTE spectrum synthesis code MOOG by C. Sneden (1973). MOOG compares the measured equivalent width of a given unblended line with the equivalent width calculated for a given atmospheric model. A detailed computation of the equivalent width of each individual line as a function of the abundance of the atom under consideration is carried out. For a given stellar model, the abundance is modified until the computed equivalent width matches with that of the observed equivalent width. We have used the driver abfind to derive the abundances of various elements in MOOG. The input to the code are the model atmosphere and the line list of the program star which comprises the wavelength of the line, lower excitation potential of the line, the oscillator strengths *gf* values and the measured equivalent width of the line and the atomic number of the element under consideration. MOOG basically solves the problem of radiative transfer for the spectral lines under the LTE assumption and calculates the line depth and hence the theoretical equivalent widths.

Atomic data

For any abundance analysis, the *gf* values are very crucial for computing accurate abundances for various elements. For the light elements C, N, O and other elements like Na, Mg, Al, Si, S, Ca, Sc, Ti, Cr, V, Mn, Cu, Co and Ni we have taken the *gf* values from the critical compilation given in the NIST database. For elements like Zn, Sr, Ba we have made use of the compilation given by Luck. For Fe I – (Fuhr and Wiese, 2006, J. Phys. Chem. Ref. Data, 35, 1669), Fe II – (Meléndez and Barbuy, 2009, A&A, 497, 611), Zr – (Biémont et al. (1981), ApJ, 248, 867), La – (Lawler et al. (2001a), ApJ, 556, 452), Ce – (Lawler et al. (2009), ApJS, 182, 51), Pr and Dy – (Sneden et al. (2009, ApJS, 182, 80), Nd – (Den Hartog et al. (2003), ApJS, 148, 543), Sm – (Lawler et al. (2006), ApJS, 162, 227), Eu – (Lawler et al. (2001b), ApJ, 563, 1075).

Determination of the Stellar parameters

a) The microturbulence (ξ_t) is derived by requiring that the derived abundances are independent of line strengths. In most of the cases Fe II lines have been used to

[2]http://kurucz.harvard.edu/grids.html (see also Castelli and Kurucz 2003)

derive ξ_t since appreciable departures from LTE are known to occur for Fe I lines.

b) The effective temperature T_{eff} is estimated by requiring that the derived abundances are independent of the lower excitation potential. For hotter stars Fe II lines and for cooler stars Fe I lines were used for the estimation of T_{eff}.

c) The surface gravity *log g* is derived by requiring Fe I and Fe II to give the same abundance. In addition the ionisation balance between Mg I/ Mg II. Si I/Si II, Ti I/Ti II, Cr I/Cr II were used as additional constraints whenever possible.

Results:

a) Chemical Compositions of RV Tauri and related objects

We present a comprehensive abundance analysis for seven unexplored RV Tauri and RV Tauri like stars using high resolution spectra. Among them IRAS 06165+3158 (see Figure 9) and V820 Cen show indications of mild s-processing which is not commonly seen among RV Tauri stars. TX Per, SU Gem, IRAS 19135+3937 and BT Lac show effects of mild dust-gas winnowing. No abundance peculiarities are seen in IRAS 01427+4633. An extensive abundance analysis has also been conducted for the known RV Tauri star V453 Oph and HD 52961 showing the RVb phenomenon in its light curve (see Figure 10 for the depletion curve of HD 52961).

We have compiled stellar parameters and elemental abundances for RV Tau and Post-AGB stars studied so far. We have divided the compilations into subgroups such as those showing s-process enhancement, dust-gas winnowing, FIP effect or showing normal compositions. We find that a significant fraction of PAGBs show strong enhancement of s-process elements but the effect is not common among RV Tauris and only a few RV Tau stars exhibit weak s-process enrichment. This effect (for PAGBs as well as for RV Tauris) is prevalent only in single stars.

A sizable number of PAGBs (a good fraction of them have binary detection) exhibit strong signature of dust-gas winnowing; however dust-gas winnowing is seen in a very large sample of RV Tau stars (with or without binary detections). The extended sample of RV Tauris showing dust-gas winnowing has resulted in identifying different kinds of slopes and structures in the depletion plots. We have attempted explaining these observed families of depletion plots in the framework of different star− circumstellar material geometries, the temperature and the composition of dust-gas reservoir, as well as the degree of mixing between the accreted clean gas with the atmosphere/envelope of the star.

• It is likely that the size of depletion depends on the mixing; When the mixing

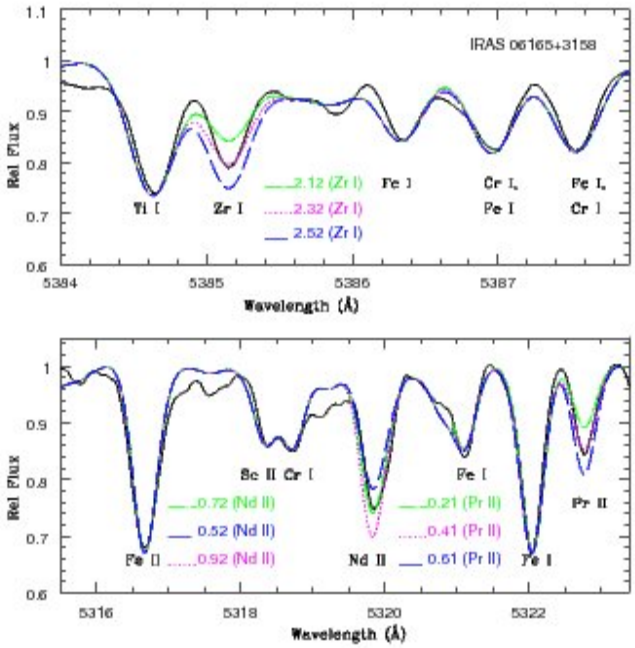

Figure 9: The agreement between synthesised and observed spectrum for IRAS 06165+3158.

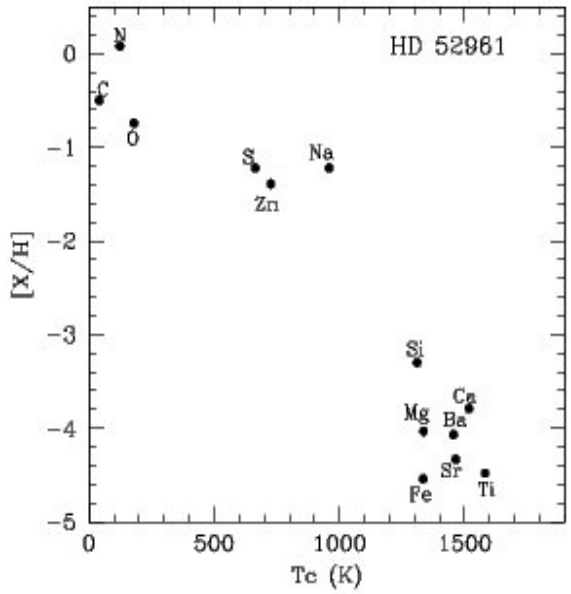

Figure 10: Plot of [X/H] versus T_C for HD 52961

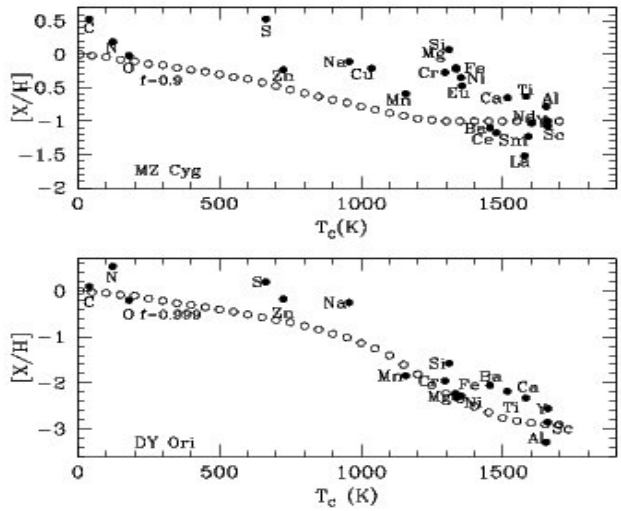

Figure 11: The observed data points are compared with the depletion predictions made using the mixing fraction giving the best fitting curve for the observed depletion plots for MZ Cyg and DY Ori.

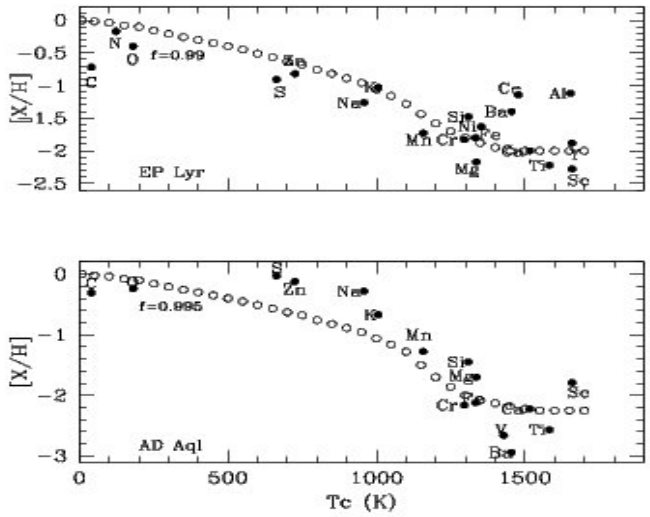

Figure 12: The observed data points are compared with the depletion predictions made using the mixing fraction giving the best fitting curve for the observed depletion plots for EP Lyr and AD Aql.

fraction f=0.9999, the stellar photosphere develops almost the same composition as that of the interstellar gas. As the mixing fraction decreases, the severity of the depletion decreases as well the depletion curves asymptotes at higher T_C. This

model however can explain only few PAGB's and RV Tauri's with depletion plots that exhibit asymptotic behaviour for the high T_C elements. For example: AD Aql (f=0.995) and EP Lyr (f=0.99) (see Figure 12), DY Ori (f=0.999) and MZ Cyg (f=0.9) (see Figure 11).

• The depletion plots are also affected by conditions of dust-gas reservoir. The extreme case of R Sct with almost a precipice like depletion plot (see Figure 13) is found to deviate from the ISM values possibly due to its warmest circumstellar dusty environment compared to other program RV Tauri stars.

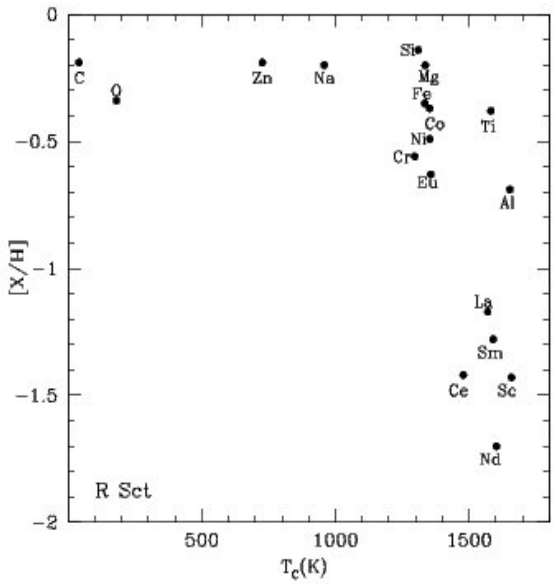

Figure 13: Plot of [X/H] versus T_C for the RV variable: R Sct. The values of [X/H] are from Giridhar, Lambert and Gonzalez (2000)

b) Chemical Composition of a sample of candidate post-AGB stars

We have derived elemental abundances for a sample of nine IRAS sources with colours similar to those of post-AGB stars. For IRAS 01259+6823, IRAS 05208-2035, IRAS 04535+3747 and IRAS 08187-1905 this is the first detailed abundance analysis based upon high resolution spectra.

• Earlier studies of post-AGB stars had led to the discovery of two classes of objects: one with large [s/Fe] in the range +1.5 to +2.3 and led to the phrase "have" and the other class of objects "have not" meaning those with [s/Fe]~0. But for the first time we find moderate s-process enhancements with [s/Fe]~0.30

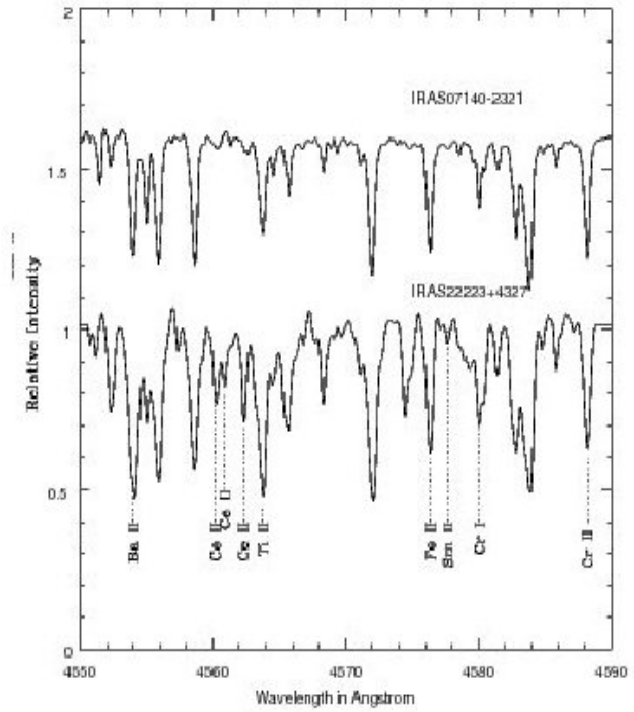

Figure 14: The spectrum of s-process enhanced object IRAS2223+4327 alongwith with IRAS07140-2321 without s-process enhancement.

in three of our program stars: IRAS 01259+6823, IRAS 05208-2035 and IRAS 08187-1905 .

• A comprehensive study of the s-process enhanced objects IRAS 17279-1119 and IRAS 22223+4327 has also been carried out. Figure 14 shows the spectra of these s-process enriched stars in comparison with a normal star of a similar temperature in the 4550-4590Å region. The lines of the s-process elements like Ba II, Ce II and Sm II are clearly enhanced.

• We have also made a contemporary abundance analysis of the high galactic latitude supergiants BD+39^o 4926 and HD 107369. The former is heavily depleted in refractories and estimated [Zn/H] of -0.7 dex most likely gives initial metallicity of the star as can be seen in the Figure 15. For HD 107369 the abundances of α and Fe-peak elements are similar to those of halo objects and moderate deficiency of s-process elements is seen.

• We have compiled the stellar parameters and abundances for post-AGB stars with s-process enhancement, those showing significant depletion of condensable elements and those showing neither. The compilation shows that the s-process enhanced group contains very small number of binaries, and observed [α/Fe] are

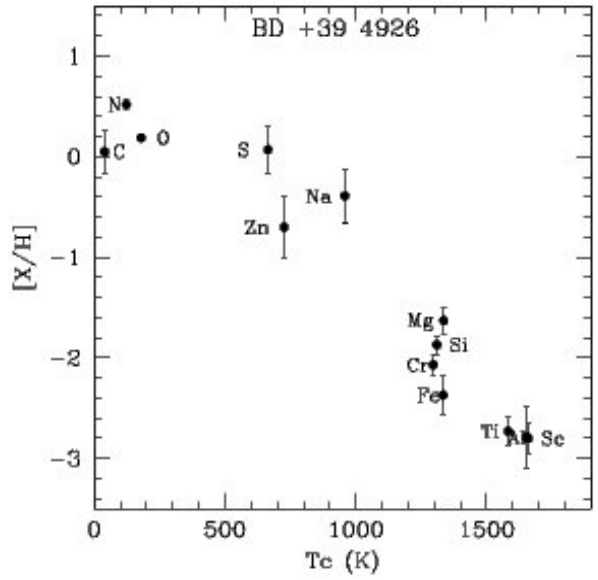

Figure 15: Depletion plot for BD+39^o 4926

generally similar to thick disc values. It is likely that they represent AGB evolution of single stars.

• The compilation of depleted group contains larger fraction of binaries and generally supports the hypothesis of dusty discs surrounding binary post-AGB stars inferred via the shape of their SED and mid IR interferometry. IRAS 07140-2321 and BD+39^o 4926 are difficult to explain with this scenario and indicate the existence of additional parameter/condition needed to explain the depletion phenomenon. However the conditions for discernible depletion, minimum temperature of 5000K and initial metallicity larger than -1.0 dex found from our earlier work still serves as useful criteria.

• **Intriguing Objects:**

a) BD+39^o 4926 : is a post-AGB binary showing strong effects of d-g separation but does not show signature of a circumstellar dust shell (IR excess) which is expected if the star is a part of a binary system.

b) IRAS 07140-2321: is a short period (116d) binary with detected circumstellar material but does not show any effects of dust-gas winnowing.

Thus it appears that the processes involved for the effective dust-gas winnowing are not fully understood.

Paper:3 Is SAO40039 a mildly H-deficient star ?

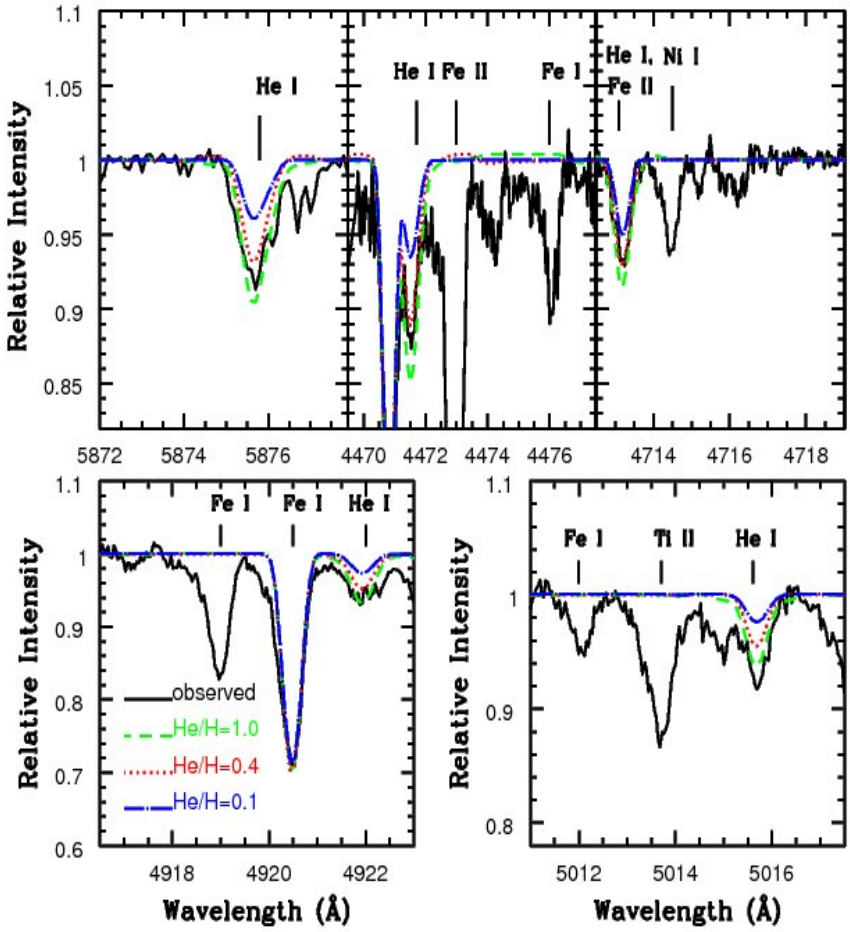

Figure 16: The observed and synthesized He I profiles for the triplet lines at 5876, 4471 and 4713Å and for the singlet lines at 4922 and 5015Å for SAO 40039 using models with$T_{\rm eff}$ = 8000K, log g = 0.75 for He/H = 1.0, 0.4 and 0.1 – see keys on the figure.

One of our program stars, SAO 40039 turned out to be a very exotic object. The spectrum of the warm post-AGB star SAO 40039 showed surprisingly strong He I lines for its effective temperature and hence has been suspected of being H-deficient and He-rich. This is the first detection of a mildly hydrogen deficient star. High-resolution optical spectra are analyzed using a family of model atmospheres with different He/H ratios. Atmospheric parameters are estimated from the ionization equilibrium set by neutral and singly ionized species of Fe and Mg,

the excitation of Fe I and Fe II lines, and the wings of the Paschen lines. On the assumption that the He I lines are of photospheric and not chromospheric origin, a He/H ratio of approximately unity is found by imposing the condition that the adopted He/H ratio of the model atmosphere must equal the ratio derived from the observed He I triplet lines at 5876, 4471 and 4713Å , and singlet lines at 4922 and 5015Å as can be seen in Figure 16.

Using the model with the best-fitting atmospheric parameters for this He/H ratio, SAO 40039 is confirmed to exhibit mild dust-gas depletion, i.e., the star has an atmosphere deficient in elements of high condensation temperature.

The star appears to be moderately metal-deficient with [Fe/H]=−0.4 dex. But the star's intrinsic metallicty as estimated from Na, S and Zn, elements of a low condensation temperature, is $[Fe/H]_o$[3]$=\simeq -0.2$. The star is enriched in N and perhaps O too, changes reflecting the star's AGB past and the event that led to He enrichment.

SUMMARY OF THE WORK DONE

In our study of RV Tauri stars and other post-AGB candidates, we have conducted detailed abundance analysis using high resolution spectra of a sample of 13 RV Tauri stars and 8 post-AGB candidates.

• From the abundance analysis of RV Tauri stars we find indications of mild s-processing in V820 Cen and IRAS 06165+3158. This s-process enrichment is a rare-phenomenon in the galactic RV Tauri stars. Till now only one galactic RV Tauri star, V453 Oph has been known to show s-process enrichment. A mild suggestion of dust-gas winnowing is seen in the RV Tauri stars TX Per, SU Gem, IRAS 19135+3937 and BT Lac. A more extensive analysis of the heavily depleted RV Tau object HD 52961 has also been conducted.

• From our analysis of post-AGB candidates for the first time we report moderate s-process enrichment ([s/Fe∼0.30) in three stars: IRAS 01259+6823, IRAS 05208-2035 and IRAS 08187-1905. All these objects being metal-poor the moderate s-process enrichment may be caused by fewer thermal pulses experienced by relatively low mass stars but dredged up to the surface via efficient mixing of nucleosynthesis product in the metal-poor environment. We have also come across two intriguing objects BD+39^{o}4926 (a post-AGB binary showing strong effects of dust-gas winnowing but without any detected IR excess) and IRAS 07140-2321 (a short period binary with detected IR excess but which does not show effects of dust-gas winnowing) pointing to the inadequacy of proposed boundary conditions associated with the dust-gas effect.

[3] $[Fe/H]_o$ refers to the star's intrinsic metallicity

• We have compiled the stellar parameters and abundances for RV Tau stars and post-AGB candidates with s-process enhancement, those showing the effects of dust-gas winnowing and those showing neither of these effects. The compilation shows that the s-process enhanced group contains very small number of binaries and probably represent AGB evolution of single stars. The depleted group contains large fraction of binaries and supports the hypothesis of dusty discs surrounding binary post-AGB stars via the shape of their SED and mid IR interferometry. The conditions for discernible depletion, minimum temperature of 5000K and initial metallicity larger than -1.0 dex found from the earlier work still serve as useful criterion.

• We have also attempted to explain the observed families of depletion plots in the framework of different star− circumstellar material geometries, the temperature and the composition of dust-gas reservoir, as well as the degree of mixing between the accreted clean gas with the atmosphere/envelope of the star.

• In our sample of PAGB candidates we also came across an exotic object: SAO 40039 a warm post-AGB star showing strong He I lines. We determined spectroscopically the He/H ratio of 1.0 which is greater than the solar He/H value of 0.1. This is the first detection of a mildly hydrogen-deficient star. The mild hydrogen deficiency would have resulted from the partial removal of the hydrogen-rich convective envelope during a late thermal pulse.

References

[] Alcock, C., Allsman, R. A., Alves, D. R. et al., 1998, AJ, 115, 1921

[] Castelli, F., Kurucz, R. L., 2003, in Piskunov, N., Weiss, W. W., Gray, D. F., eds, Proc. IAU Symp. 210, Modelling of Stellar Atmospheres, ASAP, San Francisco, p.A20

[] Gingold, R. A., 1985, MmSAI, 56, 169

[] Giridhar, S., Lambert, D. L., Gonzalez, G., 2000, ApJ, 531, 521

[] Herwig, F., 2005, ARA&A, 43, 435

[] Jura, M., 1986, ApJ, 309, 732

[] Karakas, A. I., 2010, in Principles and Perspectives in Cosmochemistry, Springer-Verlag Berlin Heidelberg,A&SS Proc Vol. ISBN 978-3-642-10351-3, p.107, A. Goswami and B. E. Reddy eds.

[] Kukarkin, B. V., Parenago, P. P., Kholopov, P. N., 1958, General Catalogue of Variable Stars, 2nd edn. Academy of Sciences of USSR, Moscow

[] Lattanzio, J. C., Boothroyd, A. I., 1997, in Astrophysical implications of the laboratory study of presolar materials, Missouri (USA), p.85, AIP Conf. Proc. Ser. Vol.402, T. J. Bernatowicz and E. Zinner eds.

[] Lloyd Evans, T., 1985, MNRAS, 217, 493

[] Lloyd Evans, T., 1999, IAU Symp No. 191, p.453

[] Maas, T., Van Winckel, H., Lloyd Evans, T., 2005, A&A, 429, 297

[] Maas, T., Van Winckel, H., Waelkens, C., 2002, A&A, 386, 504

[] Nook, M. A., Cardelli, J. A., Nordsieck, K. H., 1990, ApJ, 100, 2004

[] Pollard, K. R., Cottrell, P. L., Kilmartin, P. M., Gilmore, A. C., 1996, MNRAS, 279, 949

[] Preston, G. W., Krzeminski, W., Smak, J., Williams, J. A., 1963, ApJ, 137, 401

[] Rao, N. K., Reddy, B. E., 2005, MNRAS, 357, 235

[] Rao, N. K., Sriram, S., Jayakumar, K., Gabriel, F., 2005, JA&A, 26, 331

[] Raveendran, A. V., 1989, MNRAS, 238, 945

[] Reyniers, M., 2002, Ph.D Thesis, K. U. Leuven

[] Romano, D., Karakas, A. I., Tosi, M., Matteucci, F., 2010, A&A, 522, A32

[] Sneden, C., 1973, Ph.D Thesis, Univ. of Texas at Austin, USA

[] Suárez, O., García-Lario, P., Manchado, A., Manteiga, M., Ulla, A., Pottasch, S. R., 2006, A&A, 458, 173

[] Szczerba, R., Siódmiak, N., Stasińska, G., Borkowski, J., 2007, A&A, 469, 799

[] Tull, R. G., MacQueen, P. J., Sneden, C., Lambert, D. L., 1995, PASP, 107, 251

[] van der Veen, W. E. C. J., Habing, H. J., 1988, A&A, 194, 125

[] Van Winckel, H., 2003, ARA&A, 41, 391

LIST OF PUBLICATIONS

REFEREED JOURNALS

Sumangala Rao, S., Giridhar, S., & Lambert, D. L., *Chemical Composition of a Sample of Candidate Post-AGB Stars*, 2012, MNRAS, 419, 1254

Sumangala Rao, S., Pandey, G., Lambert, D. L., & Giridhar, S., *Is the Post-AGB Star SAO40039 Mildly Hydrogen-Deficient*?, 2011, ApJ (Letters), 737, L7

POSTER PRESENTATION

Sumangala Rao, S., Giridhar, S., & Lambert, D. L., *Elemental abundances of RV Tau and related stars*, 2011, 29^{th} Scientific Meeting of ASI held at Raipur, India

TO BE SUBMITTED SHORTLY

Sumangala Rao, S., Giridhar, S., & Lambert, D. L., *Chemical Compositions of RV Tauri and Related Objects*, to be submitted to MNRAS